

Odontocete detections are linked to oceanographic conditions in the Hawaiian Archipelago

Morgan A. Ziegenhorn ¹✉, John A. Hildebrand ¹, Erin M. Oleson ², Robin W. Baird ³ & Simone Baumann-Pickering ¹

Understanding environmental drivers of species' behavior is key for successful conservation. Within cetacean research, studies focused on understanding such drivers often consider local conditions (e.g., sea surface temperature), but rarely include large-scale, long-term parameters such as climate indices. Here we make use of long-term passive acoustic monitoring data to examine relationships between eight classes of toothed whales and climate indices, specifically El Niño Southern Oscillation, Pacific Decadal Oscillation, and North Pacific Gyre Oscillation, as well as local surface conditions (temperature, salinity, sea surface height) at two sites in the Hawaiian Archipelago. We find that El Niño Southern Oscillation most influenced cetacean detections at monitored sites. In many cases, detection patterns matched well with combinations of one or more climate indices and surface conditions. Our results highlight the importance of considering climate indices in efforts to understand relationships between marine top predators and environmental conditions.

¹Scripps Institution of Oceanography, University of California San Diego, La Jolla, CA, USA. ²NOAA Fisheries Pacific Islands Fisheries Science Center, Honolulu, HI, USA. ³Cascadia Research Collective, Olympia, WA, USA. ✉email: maziegenhorn36@gmail.com

As a relatively productive oasis in the generally oligotrophic North Pacific Subtropical Gyre¹, the Hawaiian Archipelago provides a unique study site for toothed whales (odontocetes), with at least 18 species of odontocetes residing in the region². The archipelago consists of volcanic islands, separated into the Northwestern Hawaiian Islands (NWHI, older islands) and the Main Hawaiian Islands (MHI, newer islands). Oceanographic conditions in these regions differ significantly, with the MHI experiencing high nearshore upwelling³, regional fronts and leeward eddies^{4–8}, and increased mixing and turbulence in channels between islands that encourage relatively high primary productivity³. This subsequently supports a variety of odontocete prey species (e.g., myctophids, shrimp, squids, cephalopods, and demersal and mesopelagic fishes^{9–13}). Nutrient input along coastal areas from frequent rainfall and steep island slopes also promotes the flourishing of odontocete prey; this effect is concentrated nearshore on the windward side of the islands¹⁴ but more dispersed and diluted in the islands' lees due to westerly winds¹⁵. In the NWHI, the contrast between inshore and offshore production is less marked because of eddies and a lack of above-water land mass. However, proximity to the transition zone chlorophyll front (TZCF) near the Subtropical Convergence Zone also results in higher productivity and increased abundance of odontocete prey species compared to the surrounding gyre¹⁶ (Table 1). The heightened production supported by these processes provides prime habitat for many odontocete species and results in numerous island-associated populations of various species.

Both parts of the island chain are also influenced by large-scale climate events, including the El Niño Southern Oscillation (ENSO), the Pacific Decadal Oscillation (PDO), and the North Pacific Gyre Oscillation (NPGO). The ENSO cycle describes the anomalous coupling of tropical Pacific ocean-atmosphere conditions, which is naturally occurring and varies on a 4–7 year scale, with global effects (e.g. refs. 17–19). The PDO cycle varies on a 15–25 year scale, with warm and cool phases classified by anomalous surface temperatures in the North Pacific Ocean (e.g., for the 'cool' phase, a colder eastern equatorial Pacific and warmer horseshoe connecting the southern, western, and northern Pacific²⁰). The NPGO is the most recently defined of the three indices and is significantly correlated with previously unexplained fluctuations in chlorophyll-a, nutrients, and salinity in the Northeastern Pacific. This climate pattern varies on a similar scale to the PDO and reflects changes in the circulation of the North Pacific Subtropical Gyre²¹.

In the MHI, positive ENSO and PDO conditions are linked to higher sea surface temperature (SST) as well as lower sea surface salinity (SSS), deeper mixed-layer depth, lower chlorophyll-a concentrations, and lower net primary productivity²². Negative ENSO and PDO conditions are linked to opposite trends, resulting in higher productivity during negative ENSO and PDO phases (Table 1). In the NWHI, relationships to ENSO and PDO are more likely to be related to north-south movements of the TZCF. This front fluctuates seasonally and is closest to the islands during the winter (30–35° N), and furthest away in the late summer (40–45° N)²³. Positive ENSO and PDO conditions lead to southward movement of the front, resulting in higher productivity in the NWHI region; this is especially pronounced in the winter^{24,25}. This is primarily driven by the PDO but is enhanced by positive ENSO conditions²⁶. These patterns in the NWHI are driven by the tradeoff between northeasterly trade winds (which are stronger during negative ENSO and PDO phases), as opposed to stronger westerly winds during positive phases²⁶. Across the entirety of the islands, it has been noted that positive PDO causes more frequent positive ENSO events, and vice versa²⁷, further emphasizing the combined effects of these two climate indices.

Table 1 Site summary.

| Site | Location | Deployment depth range (m) | Human influence | Oceanographic dynamics | Most productive climate state ^{22,24,26,27} | | |
|---------|----------|----------------------------|-----------------|---|--|-----|------|
| | | | | | ENSO | PDO | NPGO |
| Hawai'i | MHI | 550–750 | high | High relative productivity supported by upwelling ³ , fronts and eddies ^{4–8} , mixing in channels between islands ³ , nutrient input along coast ^{14,15} | – | – | + |
| Manawai | NWHI | 750–970 | low | High relative productivity supported by proximity to TZCF ¹⁶ , which is closest to NWHI during winter (30–35° N) and furthest in late summer (40–45° N) ²³ | + | + | + |

Summary of relevant information about the sites considered in this study including location, deployment depth range, relative anthropogenic impact (i.e., "human influence"), local oceanographic dynamics, and most productive state for the climate oscillations considered. Information from previous studies is cited where necessary.

Fluctuations in the NPGO seem to have the same affect across the entirety of the Hawaiian Archipelago. In this case, the positive phase is related to faster currents in the North Pacific Subtropical Gyre, which results in lower SST in Hawai'i²⁸. In addition, positive NPGO conditions have been related to higher SSS and mixed-layer depth as well as higher net primary productivity²², with the opposite being true for negative NPGO conditions (Table 1). These fluctuations in productivity may influence the distributions and patterns of odontocetes in the area over long timescales as they follow shifting prey distributions.

Habitat modeling has become a high-priority goal for scientists and managers in the past several decades. Using such models, scientists can become better informed about patterns of cetacean movement and their drivers. These drivers can include both intrinsic and extrinsic factors such as behavior, life-history strategies, foraging considerations, and anthropogenic influences (e.g. refs. 10,29,30). Studies of this nature often include surface variables such as SSH, SST, SSS^{31–34}, bathymetric data^{35–37}, prey-associated variables^{10,31,32}, distances to oceanographic features such as eddies^{6,38,39}, seamounts^{39,40}, or shore^{41,42}, and anthropogenic influences^{43,44}.

Previous studies in the Hawaiian region have generally obtained odontocete detections from tag data, sighting data, and limited passive acoustic data^{45–49}. However, temporal resolution of these studies has often been limited because of the methods used, resulting in little consideration of long-term climate states. An existing passive acoustic monitoring (PAM) dataset from the region covering the years 2009–2019 at sites in the MHI and NWHI provides unique opportunities to understand the relationships between both surface conditions and long-term climate indicators (ENSO, PDO, NPGO) and odontocete species in the Hawaiian Islands (Fig. 1). This dataset has been used in a previous study to extract and classify echolocation clicks⁵⁰, which are produced by odontocetes primarily while foraging and allow for identification of some species/genera. This study resulted in timeseries of eight “classes” of echolocation clicks, including five species-specific classes: false killer whale (*Pseudorca crassidens*), rough-toothed dolphin (*Steno bredanensis*), short-finned pilot whale (*Globicephala macrorhynchus*), Blainville's beaked whale (*Mesoplodon densirostris*), and Cuvier's beaked whale (*Ziphius cavirostris*), and three non-species classes: stenellid dolphins (likely including a mixed composition of pantropical spotted dolphin (*Stenella attenuata*) and spinner dolphin (*S. longirostris*), but possibly including detections of striped dolphin (*S. coeruleoalba*)²), *Kogia* spp. (primarily dwarf sperm whale (*K. sima*), but potentially containing detections of pygmy sperm whale (*K. breviceps*)⁵¹), and an unknown mix of common bottlenose dolphin (*Tursiops truncatus*), and melon-headed whale (*Peponcephala electra*)⁵⁰.

Spatiotemporal patterns in detections based on these timeseries have shown that species composition amongst sites considered was robust to season, and that temporal changes in detections varied on both diel and seasonal scales⁵². However, relationships between detections and oceanographic indicators that may provide explanations for documented patterns have not yet been assessed. Investigating relationships between oceanographic and climatological factors and odontocete presence, reflected in acoustic detections, in the islands facilitates understanding of their movement patterns over a variety of timescales. Localized shifts in odontocete presence may have significant effects on lower trophic levels due to top-down trophic effects^{53,54}. In addition to this, understanding relationships to oceanographic features is important for predicting future range shifts, responses to climate change, and in mitigating potentially harmful anthropogenic interactions such as ship strikes and fisheries bycatch. In this study, existing timeseries of odontocete detections

for the classes defined above were used in conjunction with environmental indicators to explore potential relationships. The results of this work improve upon our previous understanding of this system by investigating associations with climate indices along with more traditionally considered variables, providing novel information about odontocete responses to climate states.

Results

Modeling was completed for nearly all classes of toothed whales, excluding cases where the total number of detections was less than 100 (Table 2). Of the surface predictors considered, SSH was important in the most cases (9 class models across sites, 64%), followed by SST and SSS (4 each, 29%). ENSO and PDO were important predictors of detections for the same number of classes (9 class models, 64%) (Table 2). Explained deviance in models varied from 5% (bottlenose dolphin and melon-headed whale class off Hawai'i) to 41% (rough-toothed dolphins at Manawai). Deviance explained was higher at Manawai (5 of 7 models above 15%) than Hawai'i (4 of 7 models above 15%). Of the species considered, rough-toothed dolphins had the highest explained deviance across sites, followed by short-finned pilot whales (Table 3). The *Kogia* spp. and stenellid classes had the widest range of explained deviance, from 28% off Hawai'i to 6% at Manawai (11% and 31% for stenellids).

Hawai'i. Off Hawai'i, ENSO was the most common predictor of detections, followed by SSH, and then SST and PDO (Figs. 2 and 3). Modeling was possible at this site for all considered species except false killer whale due to limited detections (only 85 days with presence, Table 2).

Relationships to surface conditions were generally consistent in their directionality across species at this site. Detections of the bottlenose dolphin and melon-headed whale class, short-finned pilot whales, Cuvier's beaked whales, and *Kogia* spp. all had positive relationships with SSH. Conversely, all relationships to SSS were negative (rough-toothed dolphins and the bottlenose dolphin and melon-headed whale class Figs. 2 and 3). Relationships to SST were also negative, with the clearest of these being for stenellids; the final model for this group included only temperature (Figs. 2 and 3). Cuvier's beaked whales and *Kogia* spp. also had positive relationships with lower temperature conditions.

Consistency in directionality was also mostly observed for relationships to climate indices at this site. ENSO was the most included variable at this site (5 out of 7 classes) with higher detections during negative ENSO states for rough-toothed dolphins, short-finned pilot whales, and Blainville's and Cuvier's beaked whales (though for Cuvier's beaked whales there is a minimum at approximately -0.5 ENSO; Fig. 3). The exception to this relationship was *Kogia* spp. (Fig. 3). Relationships to other climate indices were less common. Both rough-toothed dolphin and *Kogia* spp. had strong positive relationships to negative PDO conditions (Figs. 2 and 3).

Manawai. At Manawai, modeling was possible for all classes except for false killer whale due to insufficient number of detections ($n = 97$). At this site, PDO was the most influential variable considered and was retained for all odontocete classes considered. ENSO and SSH were the next most common predictors, followed by SSS and SST.

Directionality of relationships to surface predictors at this site was not consistent across species (Figs. 4 and 5). SSH was the most commonly included surface predictor, with negative relationships to detections of rough-toothed dolphins and stenellids and positive relationships with Cuvier's beaked whale

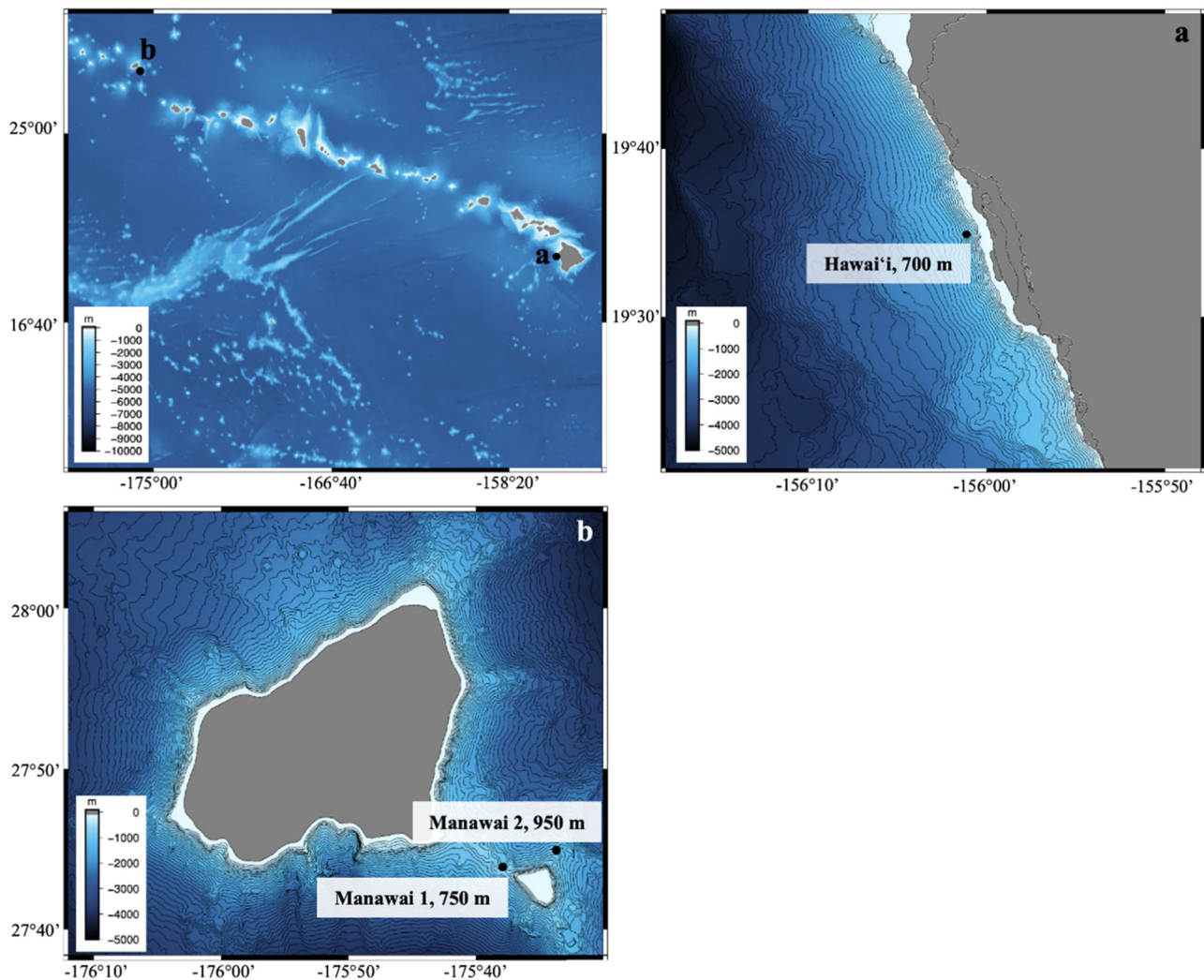


Fig. 1 Site map. Recording sites for this study, showing the location and average depth of each site, with 50 m contour lines. The non-labeled panel shows site locations in context of the Hawaiian Islands chain. Panels **a** and **b** show locations of Hawai'i and Manawai sites (respectively). Bathymetry data used for the top left panel was accessed via the General Bathymetric Map of the Ocean (GEBCO) 2022 gridded global dataset (accessible here: https://www.gebco.net/data_and_products/gridded_bathymetry_data/#global). Bathymetry data used for panels **a-b** accessed from the Hawai'i Mapping Research Group at the University of Hawai'i at Manoa (**a**, accessible here: <http://www.soest.hawaii.edu/hmrg/multibeam/bathymetry.php>) and Pacific Islands Ocean Observing System (**b**, accessible here: https://pae-paha.pacioos.hawaii.edu/thredds/bathymetry.html?dataset=hurl_bathy_60m_nwhi).

and *Kogia* spp. detections (Figs. 4 and 5). Detections of odontocetes were higher with lower SSS for the bottlenose dolphin and melon-headed whale class but increased with higher SSS for Blainville's beaked whales. Only short-finned pilot whale detections were significantly influenced by SST (higher detections with lower SST, generally; Fig. 5).

Relationships were observed between climate indices and species' detections in all cases. ENSO state was an important predictor of species' detections for all classes except the bottlenose dolphin and melon-headed whale class, short-finned pilot whales, and Cuvier's beaked whales (more detections with negative ENSO, Figs. 4 and 5). Relationships to PDO were also primarily negative, though Blainville's and Cuvier's beaked whales had a positive relationship and the *Kogia* spp. relationship was difficult to interpret (Figs. 4 and 5).

Discussion

In this study, we investigated relationships between five environmental variables and detections of eight classes of odontocetes at two sites in the Hawaiian Archipelago. Relationships to climate indices

were observed for almost all classes, with detections of nearly all classes being related to ENSO, PDO, or both. ENSO was related to detections at both sites (71% of classes off Hawai'i and 57% at Manawai), while relationships to PDO were far more common at Manawai (29%, 100% of classes, respectively) (Figs. 3 and 5).

In most cases, species' relationships to environmental variables were different at the sites considered. Of the surface variables considered, relationships to SSH may be particularly interesting, as they seem to differ for deep and shallow divers. Deep divers (e.g., beaked whales^{30,55}) had a relationship with higher SSH; the opposite was true for shallower divers (i.e., stenellids and rough-toothed dolphins^{56,57}). This seemingly holds true across sites, though off Hawai'i, SSH was only related to presence of deeper diving species.

Differential oceanographic processes at these sites may also be the cause of variability in relationships to surface conditions. At our MHI site off Hawai'i, relationships with surface variables might be driven by fluctuations in the strength or location of cold-core (e.g., productive) eddies that are known to be prevalent in the lee of the island⁸, or to localized downwelling that aggregates prey species near this site¹⁰. In the NWHI, the primary

Table 2 Model results.

| Model results (p-value, edf) | Class | Class | | | | | | |
|---------------------------------|-------|-----------------------|--------------|--------------------------------|--------------------------|---------------------------|-----------------------|--------------|
| | | Rough-toothed dolphin | Stenellids | Bottlenose d./ Melon-headed w. | Short-finned pilot whale | Blainville's beaked whale | Cuvier's beaked whale | Kogia spp. |
| Hawai'i | SSH | | | 0.046, 1 | 0.088, 1 | 0.114, 1.36 | 0.121, 1 | 0.089, 1 |
| | SSS | 0.020, 2.31 | | 0.039, 1 | | | | |
| | SST | | 0.004, 1 | | | | <0.001, 1 | 0.081, 2.13 |
| | ENSO | 0.0167, 2.63 | | | 0.027, 2.25 | 0.0391, 1 | <0.001, 2.73 | 0.060, 2.36 |
| | PDO | 0.100, 2.61 | | | | | | <0.001, 2.64 |
| Manawai | SSH | 0.02, 1.61 | 0.043, 1 | | | | 0.001, 1 | 0.204, 2.55 |
| | SSS | | | 0.029, 1 | | 0.003, 1 | | |
| | SST | | | | <0.001, 2.42 | | | |
| | ENSO | 0.004, 2.42 | 0.014, 2.71 | | | 0.041, 2.12 | 0.007, 1.05 | |
| | PDO | 0.001, 2.33 | <0.001, 2.11 | 0.003, 1.94 | 0.009, 2.07 | 0.025, 2.19 | 0.002, 2.67 | <0.001, 2.43 |

Results of final models for each species (column) and site (row) detailing significance levels of included variables. For each variable, p-value (p) and estimated degrees of freedom (edf) are given if the variable was included in the final model for that species and site.

process that may affect productivity at Manawai is the seasonal movement of the TZCF. Results for SSS and SST may indicate the relationships here; for bottlenose dolphins and melon-headed whales, and short-finned pilot whales, detections decrease during winter which may suggest movement away from the site to a particularly advantageous foraging area, potentially closer to the front itself (Figs. 4 and 5). However, during warm-weather seasons, such a shift may not be necessary or advantageous.

This explanation also serves to partially explain ENSO and PDO relationships for these classes. In these cases (as well as potentially for rough-toothed dolphins and *Kogia* spp.), we might have expected higher detections during positive ENSO and PDO conditions when local productivity should be enhanced by the closer proximity of the TZCF (Table 1). Additional correlation analysis between oceanographic conditions and climate indices seem to support this; near Manawai, there is a positive correlation between both ENSO and PDO state and satellite-derived surface chlorophyll-a values (Supplementary Note 1, Supplementary Fig. S1). However, movement to an even more productive region elsewhere could again explain this discrepancy. Blainville's and Cuvier's beaked whales present a notable exception to this. For both beaked whale species, higher seasonal occurrence during winter⁵² when the TZCF is closer to Manawai supports the conclusion that proximity of the front may explain the positive relationship seen between PDO index and detections (Figs. 4 and 5).

Off Hawai'i, detections of all classes with relationships to ENSO were higher during the negative phase, except for *Kogia* spp. All species with a relationship to ENSO had a distinct peak in detections in late 2010 and early 2011, during which negative PDO and ENSO states lined up with a positive NPGO state—likely the most productive combination of these states in the MHI (Table 1). Interestingly, there is a sudden shift in detections of rough-toothed dolphins, Blainville's beaked whales, stenellids, and *Kogia* spp. in early 2019 (decrease for Blainville's, stenellids, and *Kogia* spp., increase for rough-toothed dolphins; Fig. 2). While these shifts may be related to a concurrent shift in PDO state, it is alternatively possible that the presence or absence of a nearby offshore experimental fish farm, which unintentionally acted as a fish aggregating device, attracting both fishing vessels and rough-toothed dolphins^{58,59} may have influenced detections off Hawai'i at this time. The distinctness of this shift warrants further investigation to see whether it is related to the concurrent PDO shift, anthropogenic activities, or both.

While relationships to ENSO were common at both sites, relationships to PDO were far more common at Manawai (100% of classes) than off Hawai'i (29%). This result suggests that climate indices may be more relevant to species' modeling in the NWHI than the MHI. The reasons for this may be multifold. The additional correlation analysis undertaken in our study indicates a higher correlation between PDO and chlorophyll-a concentration (i.e., productivity) near our NWHI site than our MHI site, which may suggest a larger effect of this climate oscillation on productivity in that region (Supplemental Information). This is logical considering the origin of the PDO (northern Pacific) versus ENSO (tropical Pacific), and the relative latitude of our sites (Fig. 1). Other differences between our sites, such as depth and relative anthropogenic influence, may also play a role (Table 1). The deployment depth off Hawai'i is significantly shallower than that of Manawai (550–750 m and 750–950 m respectively, Table 1), which likely influences foraging behavior and intrinsic species composition at these sites. The shallower MHI location may be less subject to oceanographic changes related to climate oscillations than the deeper NWHI location. In addition to this, differences in behavior may also be related to relative anthropogenic influence. Very little human activity happens around Manawai, whereas the area around the Hawai'i site has a high rate of vessel traffic, fish aggregating devices, and occasional mid-frequency active sonar events^{60,61}. Human interference from these sources may provide a confounding factor in the MHI that partially masks changes related to climate oscillations.

Dissimilarities in important variables across sites may also be caused by differential behavior of island-associated populations. Many odontocetes in the Hawaiian Islands region have both recognized pelagic stocks, which are more likely to move amongst islands, as well as island-associated stocks⁶², whose movements are more localized. For species with island-associated populations (e.g., spinner dolphins, pantropical spotted dolphins, Blainville's beaked whales, false killer whales^{2,63–65}), shifts in detections may be more likely related to localized movements (e.g., inshore-offshore; north-south) rather than broad-scale movements of pelagic individuals, though some animals from pelagic populations may also use the areas near the HARP sites.

For Manawai, subsite may also have influenced results. For short-finned pilot whales and stenellids, detections before the

Table 3 Model metrics.

| Model Metrics | | Class | | | | | | | |
|---------------|------------------------|-----------------------|-----------|--------------------------------|--------------------------|---------------------------|-----------------------|------------|--|
| | | Rough-toothed dolphin | Stenelids | Bottlenose d./ Melon-headed w. | Short-finned pilot whale | Blainville's beaked whale | Cuvier's beaked whale | Kogia spp. | |
| Hawai'i | nPresDays | 555 | 1840 | 416 | 1277 | 789 | 193 | 723 | |
| | pPresDays (%) | 27.5 | 91.2 | 20.6 | 63.3 | 39.1 | 9.6 | 35.8 | |
| | AC bin | 14 | 39 | 14 | 31 | 38 | 3 | 15 | |
| Manawai | Deviance explained (%) | 21.9 | 11 | 4.9 | 17.9 | 16.1 | 8.89 | 27.7 | |
| | nPresDays | 583 | 617 | 400 | 225 | 1268 | 642 | 142 | |
| | pPresDays (%) | 42.6 | 45.0 | 29.2 | 16.4 | 92.6 | 46.9 | 10.4 | |
| | AC bin | 17 | 11 | 28 | 5 | 16 | 7 | 2 | |
| | Deviance explained (%) | 40.5 | 31.3 | 22.4 | 28.1 | 22.8 | 12.1 | 5.77 | |

Evaluation metrics and information about final habitat models for each species (columns) and each site (rows). Metrics given are number of days with detections (nPresDays), percentage of recording days with presence (pPresDays), number of days binned to account for autocorrelation (ACbin), and deviance explained by the final model.

2012–2014 gap in data are much higher. As mentioned in the methods section, exact location of the Manawai site shifted during this data gap. Additional data from the newer subsite (i.e., Manawai 2) may illuminate whether presence of these species is truly related to the environmental variables investigated here or caused by small spatial-scale site preferences. It is also worth noting that this study models only species detections as defined by echolocation clicks, though absence of detections does not necessarily mean absence of animals. Our focus on echolocation clicks unavoidably limits our modeling to primarily foraging-based behavior. This is partially the reason why variables that impact prey are the most likely candidates for impacting species detections. Incorporation of other vocalizations produced by odontocetes (e.g., whistles, buzzes, burst pulses) into similar models would contribute to fully describing acoustic presence patterns of the species considered in relation to environmental variables.

Insights into how climate indices directly affect prey would likely improve interpretation of the patterns observed. A recent example of the utility of such information also comes from the false killer whale. This species forages commonly on epipelagic fish with active fisheries, including skipjack tuna (*Katsuwonus pelami*), yellowfin tuna (*Thunnus albacares*), and bigeye tuna (*Thunnus obesus*). Both skipjack and bigeye tuna may be more common near the MHI during the El Niño phase of ENSO^{18,66}. For yellowfin tuna, catch per unit effort in the Pacific has been previously positively correlated with PDO and negatively correlated with NPGO, on a 1–5 year lag⁶⁷. These trends suggest that positive ENSO and PDO, and negative NPGO, might provide the best foraging conditions for false killer whales who are known to feed on these tuna species⁴. While these species are not common prey for other odontocetes in the region⁶⁸, detailed future studies of other prey species' responses to climate variations could provide similarly useful insights into the patterns of presence observed in this paper.

Other contemporary habitat models provide useful context on the utility and limitations of our study. While our explained deviances are fairly low, this is often the case for GAM modeling of cetaceans, potentially due to higher numbers of false absences (possible in both sighting and acoustic data collection), or the lack of ability to use direct predictors such as prey distribution data⁶⁹. Across the globe, deviance explained in models built for odontocetes is highly variable, generally ranging from 5–70%, with many deviances below 50% (e.g. ^{69–71}). The most recent habitat models available for Hawaiian odontocetes range from 12% explained deviance for sperm whales to 56% for bottlenose dolphins⁷². While it is true that the low explained deviances in our models mean that predicted habitat presence based on our model would potentially be a poor estimate of true habitat use, it does not suggest that there is nothing to be learned from the relationships represented. Our models do provide insight into the relationships between odontocete presence and both short and long-term fluctuations in their oceanographic surroundings, which may be worth considering in more traditional, spatially based habitat models.

Available literature for habitat modeling of cetacean species primarily focuses on predictive modeling of suitable habitat across a wide spatial extent, usually with temporally-limited data (often visual survey data, e.g. refs. ^{73–75}). Such studies rarely provide descriptions of the directionality of relationships to environmental variables, and often emphasize the importance of spatially varying dynamics such as distance to shore, depth, or bathymetric features. While the importance of such variables is likely temporally robust, the exact relationships and, hence, the habitat predicted, may vary on both the short and long-term scales that have shown to be relevant to fixed-in-

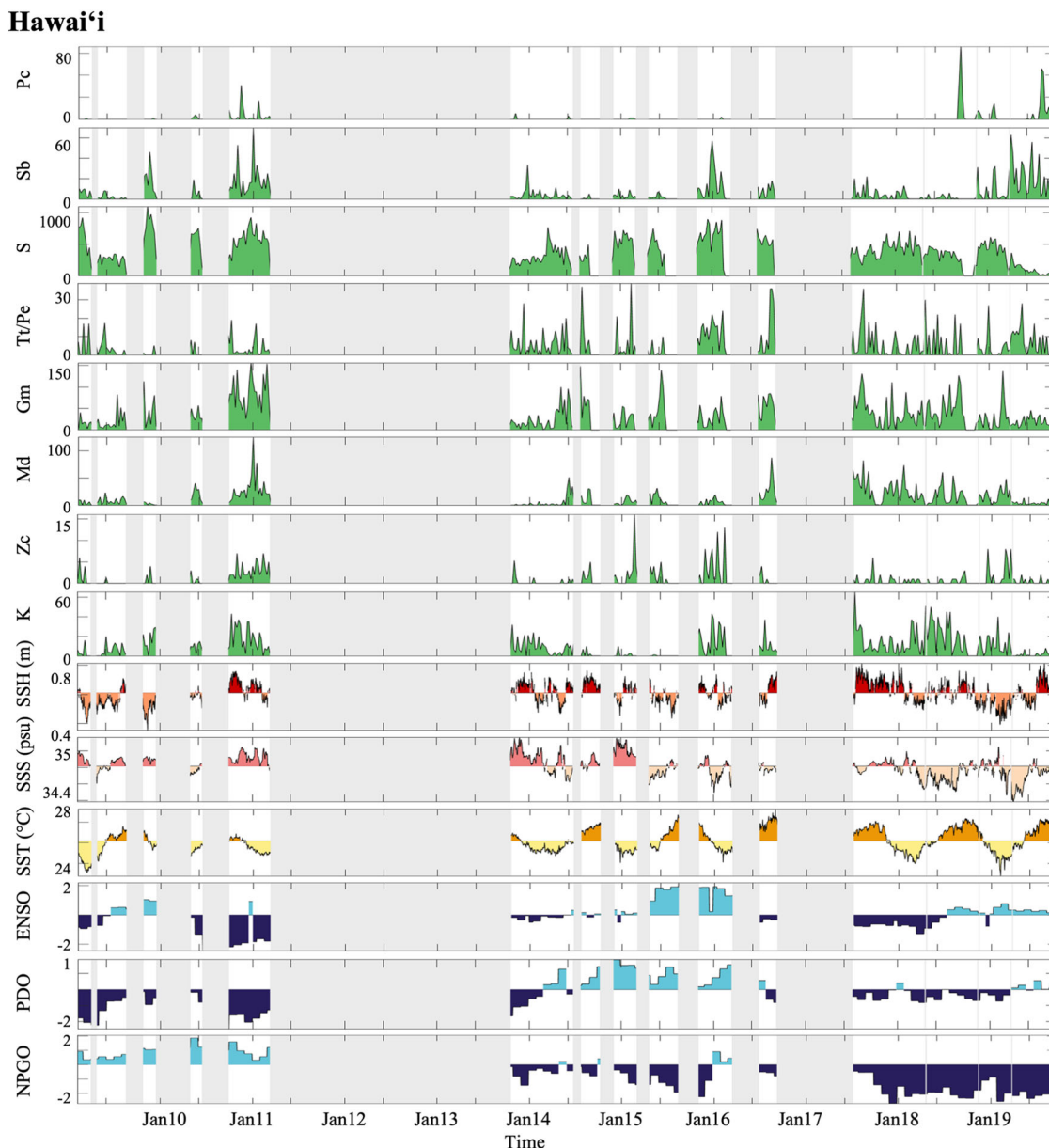


Fig. 2 Hawai'i timeseries. Timeseries of species detections in counts/week and explanatory variables off Hawai'i. Times of no effort are shown in gray. Color for each variable refers to values above or below the average value of that variable (SSH, SSS, and SST), or to positive or negative values (ENSO, PDO, NPGO). Species codes are Pc = false killer whale, Sb = rough-toothed dolphin, S = stenellids, Tt/Pe = bottlenose dolphin and melon-headed whale, Gm = short-finned pilot whale, Md = Blainville's beaked whale, Zc = Cuvier's beaked whale, and K = *Kogia* spp.

space detections used in our study. Variations in important predictor variables and hence predicted use areas have been previously observed on seasonal scales for cetaceans off the coast of southern California⁷¹. Spatial use and migration timing have also been markedly different for humpback whales in the Atlantic sector of the Southern Ocean in response to ENSO oscillations affecting local conditions (e.g., krill productivity, sea ice extent⁷⁶). In the Indian Ocean, abundance of yellowfin tuna has been linked to the combined effects of the PDO and the Southern Oscillation Index⁷⁷. This likely has associated effects on abundance and distributions of predator species in the region, which include pantropical spotted dolphins and humpback whales⁷⁸. Such results suggest that important environment may shift on both seasonal and long-term scales, illuminating the potential risk of 'snapshot' modeling of important habitats.

As mentioned in the introduction to this study, few records of odontocete changes in relation to climate indices exist. However, a recent study of false killer whales in the MHI noted that depredation of catch from long-line fisheries is higher during El Niño conditions (11 month lag), suggesting that the food web may be altered during such times⁴⁰. It has also been noted that nearshore movements of satellite-tagged false killer whales were more common during positive PDO phases in the MHI, although the relationship with PDO only explained a small amount of variance⁴⁹. Both results support the idea that predicted use areas for this species and others may be significantly different during different climate states. This may be particularly true at our NWHI site, where climate indices were significant predictors of presence in all models. As the timing and intensity of climate oscillations themselves continue to vary in relation to climate change^{79–81}, modeling predicted habitats for these species may become even more nuanced.

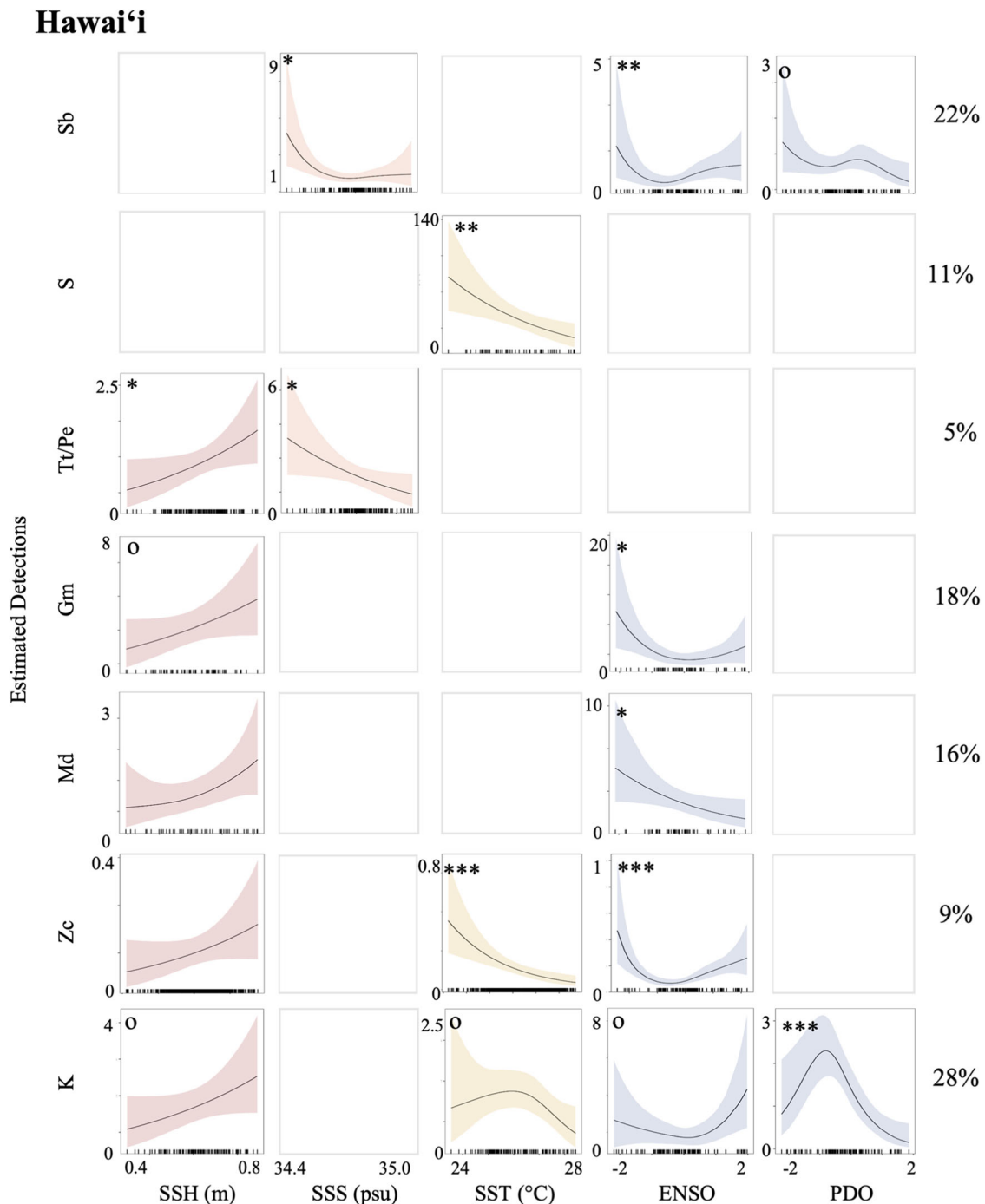


Fig. 3 Model results for Hawai'i. Partial fit smooths for all variables (columns) and each species (rows) off Hawai'i. Estimated detections for each variable are shown on y-axes in counts of 5-min bins per day. Significance level is given by ^o for $p < 0.1$, * for $p < 0.05$, ** for $p < 0.01$, *** for $p < 0.001$. Color indicates variable type (red/orange = surface, blue = climate). Column on the right shows explained deviance for each model. Species codes are Sb = rough-toothed dolphin, S = stenellids, Tt/Pe = bottlenose dolphin and melon-headed whale, Gm = short-finned pilot whale, Md = Blainville's beaked whale, Zc = Cuvier's beaked whale, and K = *Kogia* spp. False killer whales were excluded due to small sample size.

Conclusions

Significant relationships with climate indices were found for many species of odontocetes and warrant more study in the Hawaiian Islands, particularly in the NWHI. The phenomena considered (i.e., ENSO, PDO) can have long-lasting effects on environmental conditions, and subsequent effects on species behavior and movements might inform management decisions, stock assessments, and other research efforts during differing climate phases. The most striking example of this in our data

comes from the strong La Niña event of 2010, which corresponded with spikes in detections of many species at both sites. While we present an investigation of climate indices in relation to detections of odontocetes, longer timeseries from both sites would be highly useful in further examining relationships to these long-lasting climate oscillations. Ideally, future studies would include several cycles of these indices. Differing modeling frameworks might also be used to avoid correlation amongst climate states so that removal of variables (e.g., NPGO here) is not necessary.

Manawai

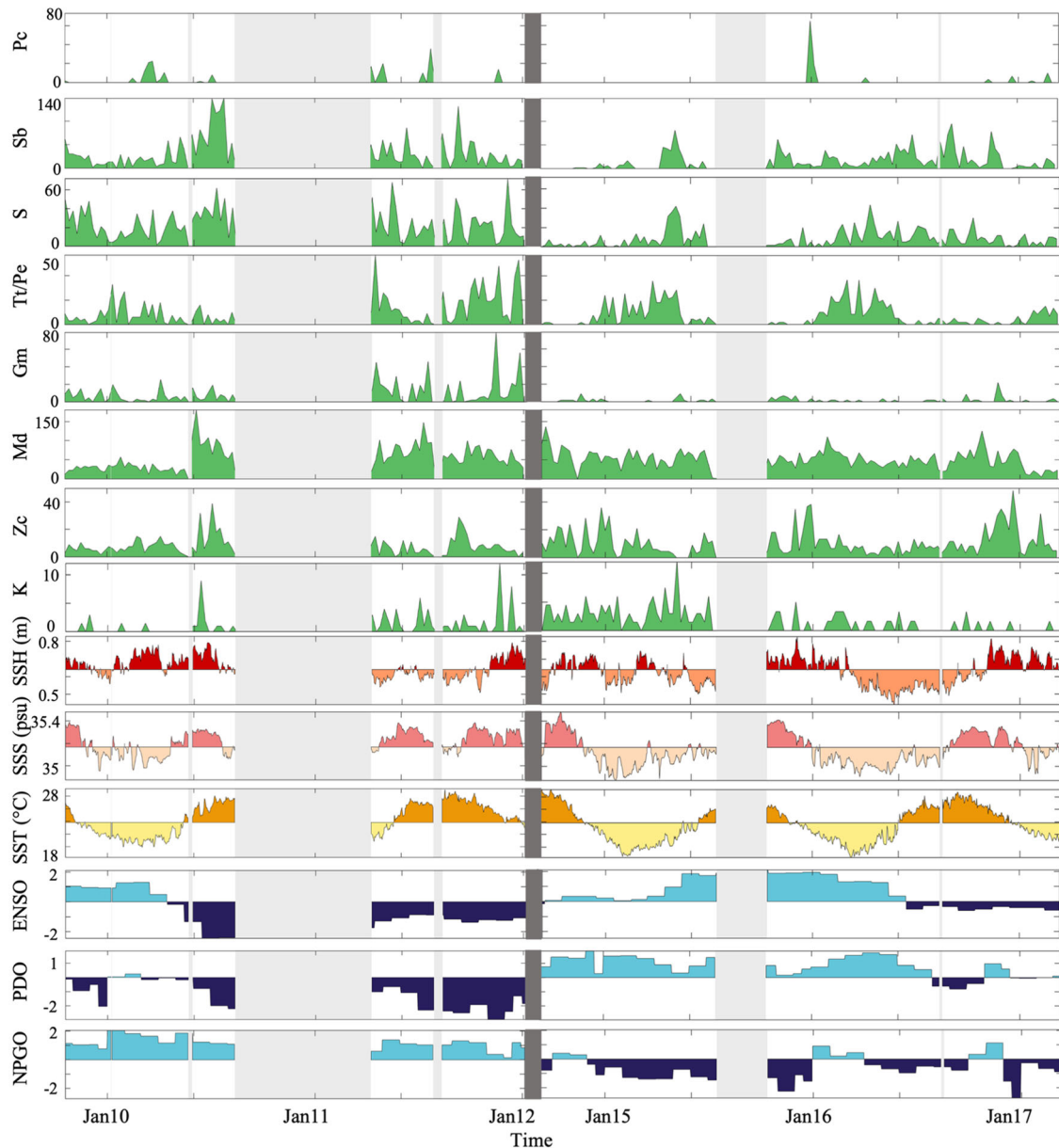


Fig. 4 Manawai timeseries. Timeseries of species detections in counts/week and explanatory variables at Manawai. Times of no effort are shown in gray; dark gray indicates the longer data gap in which site location shifted. Color for each variable refers to values above or below the average value of that variable (SSH, SSS, and SST), or to positive or negative values (MEI, PDO, NPGO). Species codes are Sb = rough-toothed dolphin, S = stenellids, Tt/Pe = bottlenose dolphin and melon-headed whale, Gm = short-finned pilot whale, Md = Blainville's beaked whale, Zc = Cuvier's beaked whale, and K = *Kogia* spp.

Overall, this study provides a novel investigation, to the best of our knowledge, of the effect of climate oscillations on detections of a variety of odontocetes in both the MHI and NWHI. Our results indicate that such oscillations may provide useful explanations for long-term fluctuations in species' presence that might be otherwise unexplained by comparable modeling efforts. In addition to this, our models highlight that differing climate states may be an important consideration for spatially extensive models aimed at predicting crucial use areas for target species, as these use areas may differ during different climate states. This may be particularly important as climate change continues to influence both the timescale, intensity, and predictability of these oscillations^{79–81}. In addition to this, differences in important predictors between sites for a given species (e.g., the importance

of SSH and ENSO for short-finned pilot whales off Hawai'i, but neither of these at Manawai) may highlight the importance of considering spatial variability in species' habitat preferences, even within a relatively small region. This is perhaps particularly important in regions like the Hawaiian Islands, where multiple disparate populations of a given species may share the area and have variable behavior.

The patterns documented are the first step towards understanding relationships of odontocetes in this region to climate indices and highlight that the combination of highly variable surface conditions and large-scale climate indices can provide unique insights into species detection patterns. Understanding these details provides another puzzle piece in the complex lives of odontocetes that will hopefully illuminate future studies.

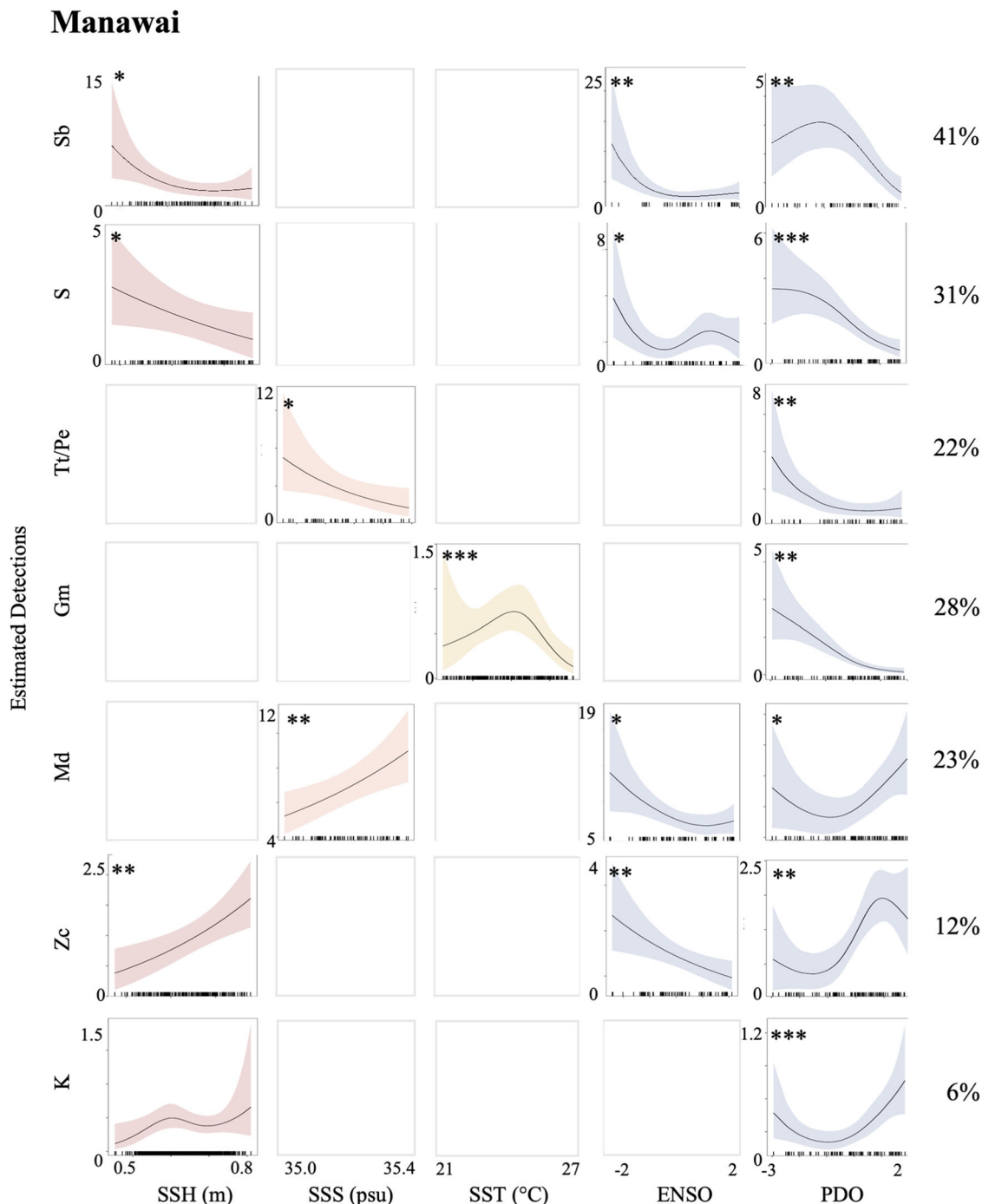


Fig. 5 Model results for Manawai. Partial fit smooths for all variables considered at Manawai (columns) for each species considered (rows). Estimated detections for each variable are shown on y-axes in counts of 5-min bins per day. Significance level is given by o for $p < 0.1$, * for $p < 0.05$, ** for $p < 0.01$, *** for $p < 0.001$. Color indicates variable type (red/orange = surface, blue = climate). Column on the right shows explained deviance for each model. Species codes are Sb = rough-toothed dolphin, S = stenellids, Tt/Pe = bottlenose dolphin and melon-headed whale, Gm = short-finned pilot whale, Md = Blainville’s beaked whale, Zc = Cuvier’s beaked whale, and K = *Kogia* spp. False killer whales were excluded due to small sample size.

Modeling habitat and understanding patterns in both space and time is crucial to preserving key spaces for these animals, mapping changes in their presence, and predicting their current and future relationships to the waters of the Hawaiian Archipelago, especially in the face of accelerating climate change.

Methods

Acoustic data collection and processing. Sites for data collection were off the west coast of Hawai’i Island (henceforth, “Hawai’i”)

and in the vicinity of Manawai, otherwise known as Holoikauaua or Pearl and Hermes Atoll (Fig. 1). In the case of Manawai, the recording site was shifted over time (approximately 10 km) to combat low-frequency hydrophone cable strumming from strong currents at depth (see “Manawai 1”, “Manawai 2”, Fig. 1b). The Hawai’i timeseries consisted of data collected from 2009–2019, while collection at Manawai 1 spanned 2009–2011 and at Manawai 2 spanned 2014–2017 (Supplementary Table S1). High Frequency Acoustic Recording Packages (HARPs) were used to

record passive acoustic data at these sites⁸². For some deployments, duty cycling (i.e., alternating periods of recording and non-recording) was employed to extend battery life and allow for longer deployments. Recording setup (e.g., duty cycle regime, instrument depth) varied over time as related projects developed (Supplementary Table S1). All data were recorded at a 200 kHz or 320 kHz sampling frequency with 16-bit quantization (see Supplementary Table S1). All hydrophones were buoyed approximately 30 m from the seafloor.

Echolocation clicks were identified in MATLAB R2020b⁸³ using an energy-based detector in the MATLAB-based software program Triton⁸⁴. This detector was run on all data to detect clicks and subsequently determine relevant click features (i.e., timing between clicks in a click train, or ‘inter-click interval’, click spectrograms, waveform envelopes). Unsupervised clustering methods were used to group clicks into echolocation click classes⁸⁵ which were identified to species or near-species (e.g., genus) level. Classes were then used to train a neural network-based classifier (using click spectrograms, inter-click interval, and waveform envelope) using a small subset of the full dataset. This classifier was implemented on all data to label acoustic detections (as defined by echolocation clicks and henceforth referred to solely as ‘detections’) as one of the identified echolocation click classes or noise^{50,86}.

Detections of all classes were binned in 5-minute increments for network training and labeling. To scale for varying degrees of false positives, class-specific precision values, a measurement of the percentage of true positive detections for a given class⁵⁰, were multiplied by numbers of clicks in 5-minute bins to approximate the number of ‘true’ clicks in that bin. Bins were retained for timeseries only if they had more than a certain number of ‘true’ clicks (>50 for delphinids, >20 for beaked whales and *Kogia* spp., based on established clicking rates for these species). Timeseries were additionally adjusted for the effect of duty cycling on both a site and class-specific basis, as duty cycling does not necessarily affect species equally⁸⁷. As detailed in ref. ⁵², timeseries of detections during continuous deployments were subsampled for each class at each site to replicate the effect of duty cycles used at that site. These subsamples were evaluated in comparison to the continuous timeseries to determine what percentage of detections would have been lost if the deployment had been duty-cycled. The resulting percentages of missed minutes per hour were used to linearly boost counts in duty cycled deployments for each class. Final timeseries presented here were re-binned into counts of 5-min bins per day for modeling purposes. Due to relatively small inter-site distance (3–10 km), similarities in acoustically detected odontocete species⁵², and to improve timeseries length, Manawai subsites were combined into a single Manawai site for analysis.

Environmental data collection and processing. Environmental variables considered in this study were related to either surface conditions (SSH, SSS, and SST) or climate indices (ENSO, PDO, and NPGO). All surface variables were acquired from the Hybrid Coordinate Ocean Model (<https://www.hycom.org/>). These variables were extracted at a daily scale on a 9 km grid from the four closest latitude-longitude points to each HARP site. Values at these points were then averaged to give one value per variable at each site per day. All climate indices were available at a monthly scale from National Oceanic and Atmospheric Administration (NOAA) databases. ENSO cycles were represented using Multivariate ENSO Index values. This index is constructed by the empirical orthogonal function of sea level pressure, SST, zonal and meridional components of surface wind, and outgoing long-wave radiation over the tropical Pacific basin and was accessed from the NOAA Physical Sciences Laboratory (<https://psl.noaa.gov/enso/mei/>). The PDO

index used is created via extended reconstruction of SST which is then compared to the Mantua PDO index and was accessed from the NOAA National Center for Environmental Information (<https://www.ncei.noaa.gov/access/monitoring/pdo/>). The NPGO index is calculated from SSH anomalies and measures changes in the North Pacific Subtropical Gyre circulation. This index was accessed via a collaboration between the National Science Foundation and the National Aeronautics and Space Administration (<http://www.o3d.org/npgo/>).

Data analysis. Habitat modeling was performed using Generalized Additive Models via the *mgcv* package in R (version 4.0.0⁸⁸) to further investigate the relationships between presence patterns and environmental variables. Models were run for each species at each site, with a negative binomial distribution to account for zero-inflation. All variables were included as smooths with four evenly spaced knots to capture non-linear relationships while avoiding overfitting³³. Correlation amongst variables was assessed using *concurvity()* in the *mgcv* package). There is no commonly accepted threshold for *concurvity* analysis, and 0.6 was chosen to remove highly correlated variables while allowing for some expected correlation between surface conditions and climate indices. Variables with *concurvity* estimates greater than this cutoff were removed from the model sequentially until all values were less than 0.6. NPGO was also removed from model analysis at this step due to its correlation with ENSO and PDO after preliminary modeling demonstrated that the two latter indices were more commonly related to species’ detections. Autocorrelation (*acf()*) in R of residuals from the full model was used to determine what level of averaging would avoid significant autocorrelation, and data were re-binned accordingly (Table 3). All possible models with remaining variables were compared using *dredge()* from the R package *MuMIn*⁸⁹ in order to determine the best final model. Models were compared at this step based on Akaike’s Information Criteria⁹⁰ for small sample sizes (AICc) value, and the model with the lowest AICc value was chosen. Partial-fit plots were created using *ggpredict()* from the *ggeffects* package in R⁹¹. For final models, deviance explained, as well as p-value and estimated degrees of freedom for each variable, were calculated using *summary()* from the *dplyr()* package in R⁹².

Reporting summary. Further information on research design is available in the Nature Portfolio Reporting Summary linked to this article.

Data availability

All data related to this manuscript can be downloaded from the following sources. Acoustic timeseries and corresponding values of environmental variables: <https://doi.org/10.5061/dryad.3n5tb2rq4> Hybrid Coordinate Ocean Model (HYCOM), for surface variables considered: <https://www.hycom.org/dataserver/gofs-3pt1/analysis> National Oceanographic and Atmospheric Administration (NOAA) Physical Sciences Laboratory, for ENSO: <https://psl.noaa.gov/enso/mei/> NOAA National Center for Environmental Information, for PDO index: <https://www.ncei.noaa.gov/access/monitoring/pdo/> National Science Foundation and the National Aeronautics and Space Administration, for NPGO index: <http://www.o3d.org/npgo/> National Aeronautics and Space Administration Moderate Resolution Imaging Spectroradiometer, for chlorophyll-a concentration: https://modis.gsfc.nasa.gov/data/dataproduct/chlor_a.php.

Code availability

Code required to reproduce models run in this study as well as Figs. 1–5 and Supplementary Figs. 1–4 can be found at <https://github.com/MZiegenhorn/Odontocetes-and-Climate> and at <https://doi.org/10.5281/zenodo.10011944>⁹³. A readme file is included which explains the purpose of each file. Code for acoustic processing to produce timeseries of odontocete detection (e.g., detection, classification) is available at <https://github.com/MarineBioAcousticsRC/Triton> and is described in more detail in^{50,52}.

Received: 20 January 2023; Accepted: 7 November 2023;

Published online: 20 November 2023

References

- Polovina, J. J., Howell, E. & Abecassis, M. Ocean's least productive waters are expanding. *Geophys. Res. Lett.* **35**, L03618 (2008).
- Baird, R. W., Webster, D. L., Aschettino, J. M., Schorr, G. S. & McSweeney, D. J. Odontocete cetaceans around the main Hawaiian Islands: Habitat use and relative abundance from small-boat sighting surveys. *Aquat. Mammals* **39**, 253–269 (2013).
- Gilmartin, M. The “island mass” effect on the phytoplankton and primary production of the Hawaiian Islands. *J. Exper. Marine Biol. Ecol.* **16**, 181–204 (1974).
- Baird, R. W. et al. False killer whales (*Pseudorca crassidens*) around the main Hawaiian Islands: Long-term site fidelity, inter-island movements, and association patterns. *Marine Mammal Sci.* **24**, 591–612 (2008).
- Seki, M. P. et al. Biological enhancement at cyclonic eddies tracked with GOES thermal imagery in Hawaiian waters. *Geophys. Res. Lett.* **28**, 1583–1586 (2001).
- Woodworth, P. A. et al. Eddies as offshore foraging grounds for melon-headed whales (*Peponocephala electra*). *Marine Mammal Sci.* **28**, 638–647 (2012).
- Bibby, T. S., Gorbunov, M. Y., Wyman, K. W. & Falkowski, P. G. Photosynthetic community responses to upwelling in mesoscale eddies in the subtropical North Atlantic and Pacific Oceans. *Deep Sea Res. Part II Top. Stud. Oceanogr.* **55**, 1310–1320 (2008).
- Calil, P. H. R. & Richards, K. J. Transient upwelling hot spots in the oligotrophic North Pacific. *J. Geophys. Res. Oceans.* **115**, C02003 (2010).
- Norris, K. S., Wursig, B., Wells, R. S. & Wursig, M. *The Hawaiian spinner dolphin* (Univ of California Press, 1994).
- Abecassis, M. et al. Characterizing a foraging hotspot for short-finned pilot whales and blainville's beaked whales located off the west side of Hawai'i island by using tagging and oceanographic data. *PLoS One* **10**, e0142628 (2015).
- Ohizumi, H., Isoda, T., Kishiro, T. & Kato, H. Feeding habits of Baird's beaked whale, *Berardius bairdii*, in the western North Pacific and Sea of Okhotsk off Japan. *Fish. Sci.* **69**, 11–20 (2003).
- West, K. L. et al. Diet of pygmy sperm whales (*Kogia breviceps*) in the Hawaiian Archipelago. *Marine Mammal Sci.* **25**, 931–943 (2009).
- West, K. L. et al. Diet of Cuvier's beaked whales, *Ziphius cavirostris*, from the North Pacific and a comparison with their diet world-wide. *Marine Ecol. Progr. Ser.* **574**, 227–242 (2017).
- Giambelluca, T. W. et al. Online rainfall atlas of Hawai'i. *Bull. Am. Meteorol. Soc.* **94**, 313–316 (2013).
- Flament, P. *The ocean atlas of Hawai'i* (University of Hawai'i, 1996).
- Schmelzer, I. Seals and seascapes: covariation in Hawaiian monk seal subpopulations and the oceanic landscape of the Hawaiian Archipelago. *J. Biogeogr.* **27**, 901–914 (2000).
- Holbrook, N. J. et al. ENSO-driven ocean extremes and their ecosystem impacts. In *El Niño southern oscillation in a changing climate*, 409–428 (American Geophysical Union, 2020).
- Howell, E. A. & Kobayashi, D. R. El Niño effects in the Palmyra Atoll region: oceanographic changes and bigeye tuna (*Thunnus obesus*) catch rate variability. *Fish. Oceanogr.* **15**, 477–489 (2006).
- Brönnimann, S. Impact of El Niño–Southern Oscillation on European climate. *Rev. Geophys.* **45**, RG3003 (2007).
- Mantua, N. J. & Hare, S. R. The Pacific decadal oscillation. *J. Oceanogr.* **58**, 35–44 (2002).
- Di Lorenzo, E. et al. North Pacific Gyre Oscillation links ocean climate and ecosystem change. *Geophys. Res. Lett.* **35**, L08607 (2008).
- Kavanaugh, M. T. et al. ALOHA from the edge: reconciling three decades of in situ eulerian observations and geographic variability in the North Pacific subtropical Gyre. *Front. Marine Sci.* **5**, 1–14 (2018).
- Polovina, J. J., Howell, E., Kobayashi, D. R. & Seki, M. P. The transition zone chlorophyll front, a dynamic global feature defining migration and forage habitat for marine resources. *Progr. Oceanogr.* **49**, 469–483 (2001).
- Polovina, J. J., Howell, E. A., Kobayashi, D. R. & Seki, M. P. The transition zone chlorophyll front updated: advances from a decade of research. *Progr. Oceanogr.* **150**, 79–85 (2017).
- Bograd, S. J. et al. On the seasonal and interannual migrations of the transition zone chlorophyll front. *Geophys. Res. Lett.* **31**, L17204 (2004).
- Wren, J. L. K., Shaffer, S. A. & Polovina, J. J. Variations in black-footed albatross sightings in a North Pacific transitional area due to changes in fleet dynamics and oceanography 2006–2017. *Deep Sea Res. Part II Top. Stud. Oceanogr.* **169–170**, 104605 (2019).
- Verdon, D. C. & Franks, S. W. Long-term behaviour of ENSO: interactions with the PDO over the past 400 years inferred from paleoclimate records. *Geophys. Res. Lett.* **33**, L06712 (2006).
- Gove, J. M. et al. West Hawai'i integrated ecosystem assessment ecosystem status report. PIFSC Special Publication. SP-19-001. (Pacific Islands Fisheries Science Center, Honolulu, Hawaii, USA, 2019).
- Forney, K. A. et al. Nowhere to go: noise impact assessments for marine mammal populations with high site fidelity. *Endangered Species Res.* **32**, 391–413 (2017).
- Baird, R. W., Webster, D. L., Schorr, G. S., McSweeney, D. J. & Barlow, J. Diel variation in beaked whale diving behavior. *Marine Mammal Sci.* **24**, 630–642 (2008).
- Kanaji, Y., Okazaki, M. & Miyashita, T. Spatial patterns of distribution, abundance, and species diversity of small odontocetes estimated using density surface modeling with line transect sampling. *Deep Sea Res. Part II Top. Stud. Oceanogr.* **140**, 151–162 (2017).
- Redfern, J. V., Barlow, J., Bailance, L. T., Gerrodette, T. & Becker, E. A. Absence of scale dependence in dolphin-habitat models for the eastern tropical Pacific Ocean. *Marine Ecol. Progr. Ser.* **363**, 1–14 (2008).
- Forney, K. A., Becker, E. A., Foley, D. G., Barlow, J. & Oleson, E. M. Habitat-based models of cetacean density and distribution in the central North Pacific. *Endanger. Species Res.* **27**, 1–20 (2015).
- Virgili, A., Racine, M., Authier, M., Monestiez, P. & Ridoux, V. Comparison of habitat models for scarcely detected species. *Ecol. Model.* **346**, 88–98 (2017).
- Thorne, L. H. et al. Movement and foraging behavior of short-finned pilot whales in the Mid-Atlantic Bight: Importance of bathymetric features and implications for management. *Marine Ecol. Progr. Ser.* **584**, 245–257 (2017).
- Azzellino, A. et al. Predictive habitat models for managing marine areas: Spatial and temporal distribution of marine mammals within the Pelagos Sanctuary (Northwestern Mediterranean sea). *Ocean Coastal Manag.* **67**, 63–74 (2012).
- Tepsich, P., Rosso, M., Halpin, P. N. & Moulins, A. Habitat preferences of two deep-diving cetacean species in the northern Ligurian Sea. *Marine Ecol. Progr. Ser.* **508**, 247–260 (2014).
- Frasier, K. E., Garrison, L. P., Soldevilla, M. S., Wiggins, S. M. & Hildebrand, J. A. Cetacean distribution models based on visual and passive acoustic data. *Scie. Rep.* **11**, 1–16 (2021).
- Roberts, J. J. et al. Habitat-based cetacean density models for the US Atlantic and Gulf of Mexico. *Sci. Rep.* **6**, 1–12 (2016).
- Fader, J. E. et al. Patterns of depredation in the Hawai'i deep-set longline fishery informed by fishery and false killer whale behavior. *Ecosphere* **12**, e03682 (2021).
- Barlow, J. & Gerrodette, T. Predicting Cuvier's (*Ziphius cavirostris*) and Mesoplodon beaked whale population density from habitat characteristics in the eastern tropical Pacific Ocean. (2006). Available from: <https://www.researchgate.net/publication/284925131>.
- Panigada, S. et al. Modelling habitat preferences for fin whales and striped dolphins in the Pelagos Sanctuary (Western Mediterranean Sea) with physiographic and remote sensing variables. *Remote Sens. Environ.* **112**, 3400–3412 (2008).
- Henderson, E. E., Martin, S. W., Manzano-Roth, R. & Matsuyama, B. M. Occurrence and habitat use of foraging Blainville's beaked whales (*Mesoplodon densirostris*) on a U.S. Navy range in Hawai'i. *Aqu. Mamm.* **42**, 549–562 (2016).
- Carlucci, R. et al. Modeling the spatial distribution of the striped dolphin (*Stenella coeruleoalba*) and common bottlenose dolphin (*Tursiops truncatus*) in the Gulf of Taranto (Northern Ionian Sea, Central-eastern Mediterranean Sea). *Ecol. Indic.* **69**, 707–721 (2016).
- Andrews, K. R. et al. Rolling stones and stable homes: Social structure, habitat diversity and population genetics of the Hawaiian spinner dolphin (*Stenella longirostris*). *Mol. Ecol.* **19**, 732–748 (2010).
- Aschettino, J. M. et al. Population structure of melon-headed whales (*Peponocephala electra*) in the Hawaiian Archipelago: Evidence of multiple populations based on photo identification. *Marine Mamm. Sci.* **28**, 666–689 (2012).
- Baird, R. W. et al. Site fidelity and association patterns in a deep-water dolphin: Rough-toothed dolphins (*Steno bredanensis*) in the Hawaiian Archipelago. *Marine Mamm. Sci.* **24**, 535–553 (2008).
- Manzano-Roth, R., Henderson, E. E., Martin, S. W., Martin, C. & Matsuyama, B. M. Impacts of U.S. Navy training events on Blainville's beaked whale (*Mesoplodon densirostris*) foraging dives in Hawaiian waters. *Aquat. Mamm.* **42**, 507–518 (2016).
- Baird, R. W., Anderson, D. B., Kratofil, M. A., Webster, D. L. & Mahaffy, S. D. Cooperative conservation and long-term management of false killer whales in Hawai'i: geospatial analyses of fisheries and satellite tag data to understand fishery interactions. Report to the state of Hawai'i Board of Land and Natural Resources. (2019).

50. Ziegenhorn, M. A. et al. Discriminating and classifying odontocete echolocation clicks in the Hawaiian Islands using machine learning methods. *PLoS One* **17**, e0266424 (2022).
51. Baird, R. W., Mahaffy, S. D. & Lerma, J. K. Site fidelity, spatial use, and behavior of dwarf sperm whales in Hawaiian waters: using small-boat surveys, photo-identification, and unmanned aerial systems to study a difficult-to-study species. *Marine Mammal Sci.* (2021). Available from: <https://onlinelibrary.wiley.com/doi/10.1111/mms.12861>.
52. Ziegenhorn, M. A. et al. Odontocete spatial patterns and temporal drivers of detection at sites in the Hawaiian islands. *Ecol. Evol.* **13**, e9688 (2023).
53. Ruzicka, J. J., Steele, J. H., Ballerini, T., Gaichas, S. K. & Ainley, D. G. Dividing up the pie: Whales, fish, and humans as competitors. *Progr. Oceanogr.* **116**, 207–219 (2013).
54. Kiszka, J. J., Woodstock, M. S. & Heithaus, M. R. Functional roles and ecological importance of small cetaceans in aquatic ecosystems. *Front. Marine Sci.* **9**, 163 (2022).
55. Tyack, P. L., Johnson, M., Soto, N. A., Sturlese, A. & Madsen, P. T. Extreme diving of beaked whales. *J. Exp. Biol.* **209**, 4238–4253 (2016).
56. Shaff, J. F. & Baird, R. W. Diel and lunar variation in diving behavior of rough-toothed dolphins (*Steno bredanensis*) off Kaua'i, Hawai'i. *Marine Mammal Sci.* **37**, 1261–1276 (2021).
57. Baird, R. W., Ligon, A. D., Hooker, S. K. & Gorgone, A. M. Subsurface and nighttime behaviour of pantropical spotted dolphins in Hawai'i. *Can. J. Zool.* **79**, 988–996 (2001).
58. Baird, R. W. *The lives of Hawai'i's Dolphins and Whales: natural history and conservation* (University of Hawai'i Press, Honolulu, Hawai'i; 2016).
59. Incorporated O. E. Ocean Era Research Projects- Offshore Technologies. 2020. Available from: <http://ocean-era.com/offshore-technologies>.
60. Selkoe, K. A., Halpern, B. S. & Toonen, R. J. Evaluating anthropogenic threats to the Northwestern Hawaiian Islands. *Aquatic Conserv. Marine Freshwater Ecosyst.* **18**, 1149–1165 (2008).
61. Merckens, K. et al. Characterizing the long-term, wide-band and deep-water soundscape off Hawai'i. *Front. Marine Sci.* **8**, 1647 (2021).
62. Carretta, J. V. et al. U.S. Pacific Marine Mammal Stock Assessments: 2020 [Internet]. (U.S.) SFSC, editor. 2021. (NOAA technical memorandum NMFS). Available from: <https://repository.library.noaa.gov/view/noaa/31436>.
63. Baird, R. W. et al. Evidence of an Island-Associated Population of False Killer Whales (*Pseudorca crassidens*) in the Northwestern Hawaiian Islands. *Pac. Sci.* **67**, 513–521 (2013).
64. Courbis, S., Baird, R. W., Cipriano, F. & Duffield, D. Multiple populations of pantropical spotted dolphins in Hawaiian waters. *J. Heredity* **105**, 627–641 (2014).
65. Baird, R. W. et al. Open-ocean movements of a satellite-tagged Blainville's beaked whale (*Mesoplodon densirostris*): Evidence for an offshore population in Hawai'i? *Aquatic Mammals* **37**, 506–511 (2011).
66. Lehodey, P. et al. Predicting skipjack tuna forage distributions in the equatorial Pacific using a coupled dynamical bio-geochemical model. *Fish. Oceanogr.* **7**, 317–325 (1998).
67. Wu, Y.-L., Lan, K.-W. & Tian, Y. Determining the effect of multiscale climate indices on the global yellowfin tuna (*Thunnus albacares*) population using a time series analysis. *Deep Sea Res. Part II Top. Stud. Oceanogr.* **175**, 104808 (2020).
68. Fader, J. E., Marchetti, J. A., Schick, R. S. & Read, A. J. No free lunch: estimating the biomass and ex-vessel value of target catch lost to depredation by odontocetes in the Hawai'i longline tuna fishery. *Can. J. Fish. Aquat. Sci.* **80**, 1121–1141 (2023).
69. Mannocci, L. et al. Predicting cetacean and seabird habitats across a productivity gradient in the South Pacific gyre. *Progr. Oceanogr.* **120**, 383–398 (2014).
70. Chavez-Rosales, S., Palka, D. L., Garrison, L. P. & Josephson, E. A. Environmental predictors of habitat suitability and occurrence of cetaceans in the western North Atlantic Ocean. *Sci. Rep.* **9**, 1–11 (2019).
71. Becker, E. A. et al. Habitat-based density models for three cetacean species off Southern California illustrate pronounced seasonal differences. *Front. Marine Sci.* **4**, 121 (2017).
72. Becker, E. A. et al. Habitat-based density estimates for cetaceans within the waters of the U.S. Exclusive Economic Zone around the Hawaiian Archipelago. (2021). Available from: <https://doi.org/10.25923/x9q9-rd73>.
73. Ferguson, M. C., Barlow, J., Fiedler, P., Reilly, S. B. & Gerrodette, T. Spatial models of delphinid (family Delphinidae) encounter rate and group size in the eastern tropical Pacific Ocean. *Ecol. Modell.* **193**, 645–662 (2006).
74. Blasi, M. F. & Boitani, L. Modelling fine-scale distribution of the bottlenose dolphin *Tursiops truncatus* using physiographic features on Filicudi (southern Tyrrhenian Sea, Italy). *Endanger. Species Res.* **17**, 269–288 (2012).
75. Bradford, A. L., Oleson, E. M., Forney, K. A., Moore, J. E. & Barlow, J. Line-transect Abundance Estimates of Cetaceans in U.S. Waters around the Hawaiian Islands in 2002, 2010, and 2017. Service. USNMF, (U.S.) PIFSC, (U.S.) SFSC, Region PI, editors. 2021. (NOAA technical memorandum NMFS-PIFSC; 115). Available from: <https://repository.library.noaa.gov/view/noaa/29004>.
76. Schall, E. et al. Multi-year presence of humpback whales in the Atlantic sector of the Southern Ocean but not during El Niño. *Commun. Biol.* **4**, 790 (2021).
77. Báez, J. C., Czerwinski, I. A. & Ramos, M. L. Climatic oscillations effect on the yellowfin tuna (*Thunnus albacares*) Spanish captures in the Indian Ocean. *Fisheries Oceanogr.* **29**, 572–583 (2020).
78. Escalle, L. et al. Cetaceans and tuna purse seine fisheries in the Atlantic and Indian Oceans: Interactions but few mortalities. *Marine Ecol. Progr. Ser.* **522**, 255–268 (2015).
79. Li, S. et al. The Pacific Decadal Oscillation less predictable under greenhouse warming. *Nat. Clim. Change* **10**, 30–34 (2020).
80. Jia, F., Cai, W., Gan, B., Wu, L. & Di Lorenzo, E. Enhanced North Pacific impact on El Niño/southern oscillation under greenhouse warming. *Nat. Clim. Change* **11**, 840–847 (2021).
81. Litow, M. A. et al. The changing physical and ecological meanings of North Pacific Ocean climate indices. *Proc. Natl Acad. Sci.* **117**, 7665–7671 (2020).
82. Wiggins, S. M. & Hildebrand, J. A. High-frequency Acoustic Recording Package (HARP) for broad-band, long-term marine mammal monitoring. In: *International Symposium on Underwater Technology, UT 2007 - International Workshop on Scientific Use of Submarine Cables and Related Technologies*. (2007). p. 551–7. Available from: <http://www.motorola.com>.
83. MATLAB. MATLAB version 9.9.0 (R2020b) (Natick, Massachusetts: The Mathworks Inc, 2020).
84. Wiggins, S. M., Roch, M. A. & Hildebrand, J. A. TRITON software package: analyzing large passive acoustic monitoring data sets using MATLAB. *J. Acoust. Soc. Am.* **128**, 2299 (2010).
85. Frasier, K. E., et al. Automated classification of dolphin echolocation click types from the Gulf of Mexico. *PLoS Comput. Biol.* **13**, e1005823 (2017).
86. Frasier, K. E. A machine learning pipeline for classification of cetacean echolocation clicks in large underwater acoustic datasets. *PLoS Computational Biology*. **17**, 1–26 (2021).
87. Stanistreet, J. E. et al. Effects of duty-cycled passive acoustic recordings on detecting the presence of beaked whales in the northwest Atlantic. *J. Acoustical Soc. Am.* **140**, EL31–7 (2016).
88. Wood, S. N. *Generalized additive models: an introduction with R* (Chapman and Hall/CRC; 2006).
89. Bartoň, K. (2023) `MuMIn`: Multi-Model Inference. R package version 1.47.5, <https://CRAN.R-project.org/package=MuMIn>.
90. Akaike, H. Information theory and an extension of the maximum likelihood principle. In *Selected papers of hirotugu akaike*. (Springer; 1998). p. 199–213.
91. Lüdecke, D. ggeffects: Tidy data frames of marginal effects from regression models. *J. Open Source Softw.* **3**, 772 (2018).
92. Wickham, H., François, R., Henry, L., Müller, K. & Vaughan, D. `dplyr`: A Grammar of Data Manipulation. R package version 1.1.2, (2023). <https://CRAN.R-project.org/package=dplyr>.
93. Ziegenhorn, M. A. Odontocete detections and corresponding values of environmental variables in the Hawaiian Archipelago. *Dryad* (2023). Available from: <https://doi.org/10.5061/dryad.3n5tb2rq4>.

Acknowledgements

A special thanks to Rebecca Cohen and Natalie Posdaljian for their input and discussions on the methods employed in this study, which had a large impact on the final product. Thank you to all members of the Scripps Whale Acoustics Lab, the Scripps Acoustic Ecology Lab, and the Scripps Machine Listening Lab for support over the course of this project. Thanks to all those at the NOAA Pacific Islands Fisheries Science Center and their partners who were involved in instrument deployment, retrieval, and work at sites used in this study. This work was funded by the NOAA Pacific Islands Fisheries Science Center Cooperative Institute for Marine Ecosystems and Climate (Grant NA15OAR43200071) and the Cooperative Institute for Marine, Earth, and Atmospheric Systems (Grant NA20OAR4320278). Manawai HARP deployments were permitted by the Papahānaumokuākea Marine National Monument under permits PMNM-2008-020 and PMNM-2010-042 and the Co-Managers permit since 2015.

Author contributions

M.A.Z. lead study conception, data analysis and processing, methodology, visualization, and manuscript writing, review, and editing (all drafts). J.A.H. contributed to conceptualization, methodology, manuscript review and editing, resources, and supervision. E.M.O. lead data collection and contributed to methodology, funding acquisition, resources, and manuscript review and editing. R.W.B. contributed to methodology and manuscript review and editing. S.B.-P. contributed to conceptualization, methodology, resources, funding acquisition, and manuscript writing, review, and editing (all drafts).

Competing interests

The authors declare no competing interests.

Additional information

Supplementary information The online version contains supplementary material available at <https://doi.org/10.1038/s43247-023-01088-7>.

Correspondence and requests for materials should be addressed to Morgan A. Ziegenhorn.

Peer review information *Communications Earth & Environment* thanks Elena Schall and the other, anonymous, reviewer(s) for their contribution to the peer review of this work. Primary Handling Editors: Clare Davis. A peer review file is available

Reprints and permission information is available at <http://www.nature.com/reprints>

Publisher's note Springer Nature remains neutral with regard to jurisdictional claims in published maps and institutional affiliations.



Open Access This article is licensed under a Creative Commons Attribution 4.0 International License, which permits use, sharing, adaptation, distribution and reproduction in any medium or format, as long as you give appropriate credit to the original author(s) and the source, provide a link to the Creative Commons licence, and indicate if changes were made. The images or other third party material in this article are included in the article's Creative Commons licence, unless indicated otherwise in a credit line to the material. If material is not included in the article's Creative Commons licence and your intended use is not permitted by statutory regulation or exceeds the permitted use, you will need to obtain permission directly from the copyright holder. To view a copy of this licence, visit <http://creativecommons.org/licenses/by/4.0/>.

© The Author(s) 2023